Since January 2020 Elsevier has created a COVID-19 resource centre with free information in English and Mandarin on the novel coronavirus COVID-19. The COVID-19 resource centre is hosted on Elsevier Connect, the company's public news and information website.

BBA Advances 2 (2022) 100044

Contents lists available at ScienceDirect

BBA Advances

journal homepage: www.sciencedirect.com/journal/bba-advances

The dynamic nature of the coronavirus receptor, angiotensin-converting enzyme 2 (ACE2) in differentiating airway epithelia

Vincent J. Manna [$], Hana Choi [*], Shawna M. Rotoli, Salvatore J. Caradonna [$]

Department of Molecular Biology, Graduate School of Biomedical Sciences and School of Osteopathic Medicine, Rowan University, Stratford, NJ, United States

ARTICLE INFO

Keywords:
Abbreviations
SARS-CoV-2, severe acute respiratory syndrome coronavirus 2
ACE2, angiotensin converting enzyme 2
sACE2, soluble/released form of ACE2
COVID-19, coronavirus disease 2019
ALI, air-liquid interface
SDS-PAGE, sodium dodecyl sulfate – polyacrylamide gel electrophoresis
RAS, renin-angiotensin system
Ang, angiotensin
HNEC, human nasal endothelial cells
hs, homo sapien
TCE, total cell extract
IP, immunoprecipitation
RpAb, rabbit polyclonal antibody
RmAb, rabbit monoclonal antibody
PNGase F, Peptide:N glycosidase F
UTR, untranslated region

ABSTRACT

Once inhaled, SARS-CoV-2 particles enter respiratory ciliated cells by interacting with angiotensin converting enzyme 2 (ACE2). Understanding the nature of ACE2 within airway tissue has become a recent focus particularly in light of the COVID-19 pandemic. Airway mucociliary tissue was generated *in-vitro* using primary human nasal epithelial cells and the air-liquid interface (ALI) model of differentiation. Using ALI tissue, three distinct transcript variants of ACE2 were identified. One transcript encodes the documented full-length ACE2 protein. The other two transcripts are unique truncated isoforms, that until recently had only been predicted to exist via sequence analysis software. Quantitative PCR revealed that all three transcript variants are expressed throughout differentiation of airway mucociliary epithelia. Immunofluorescence analysis of individual ACE2 protein isoforms exogenously expressed in cell-lines revealed similar abilities to localize in the plasma membrane and interact with the SARS CoV 2 spike receptor binding domain. Immunohistochemistry on differentiated ALI tissue using antibodies to either the N-term or C-term of ACE2 revealed both overlapping and distinct signals in cells, most notably only the ACE2 C-term antibody displayed plasma-membrane localization. We also demonstrate that ACE2 protein shedding is different in ALI Tissue compared to ACE2-transfected cell lines, and that ACE2 is released from both the apical and basal surfaces of ALI tissue. Together, our data highlights various facets of ACE2 transcripts and protein in airway mucociliary tissue that may represent variables which impact an individual's susceptibility to SARS-CoV-2 infection, or the severity of Covid-19.

Introduction

The identification of the ACE2 protein as the receptor for SARS-CoV-2 infection leads to the tenet that the efficiency of infection is causally related to the amount and nature of ACE2 available for binding [1]. The main route of transmission of SARS-CoV-2 is through respiratory droplets, once inhaled the viral particles bind to and infect proximal airway cells using a viral encoded spike protein that interacts with ACE2. ACE2 is an integral membrane-spanning protein with an extracellular domain [2,3].

In addition to providing a receptor for SARS-CoV-2 infection, ACE2 plays a very seminal role in the body. As a counterpart to ACE, ACE2 has emerged as an important co-regulator of the renin-angiotensin system (RAS) [4]. The primary role of ACE is to hydrolyze angiotensin I (Ang I) to a potent vasoconstrictor, angiotensin II (Ang II). Among its actions ACE2 cleaves Ang II to Ang (1–7), a peptide with opposing functions to Ang II that acts through its own receptor, MAS [5–7]. Ang II was originally considered as a short-acting, vasoactive hormone. Research over the years now presents Ang II as a peptide hormone that impinges on multiple signaling pathways. It can produce aberrant effects leading to cardiovascular disease with pathologies that include cardiac hypertrophy, endothelial dysfunction, fibrosis, and inflammation [8]. Accumulating evidence indicates that Ang-(1–7) can reduce the levels of pro-inflammatory cytokines such as TNF-alpha and IL-6 [9]. In addition, data from ACE2 knockout mice suggests that ACE2 plays a protective role in acute lung injury [10]. This evidence indicates that ACE2

$ Corresponding authors: Department of Molecular Biology, Rowan University, 42 East Laurel Road, Suite 2200, P.O. Box 1011, Stratford, New Jersey 08084 United States.

E-mail addresses: mannav6@rowan.edu (V.J. Manna), caradonna@rowan.edu (S.J. Caradonna).

* Current Address: Division of Hematology-Oncology, Department of Medicine, Perelman School of Medicine, University of Pennsylvania, Philadelphia, Pennsylvania 19104, United States

https://doi.org/10.1016/j.bbadva.2022.100044
Received 2 June 2021; Received in revised form 13 January 2022; Accepted 6 February 2022
Available online 12 February 2022

has a role in moderating inflammatory responses. ACE2 is also known to neutralize other vasoactive peptides such as bradykinin and related endogenous peptides [4,11]. Additional apparent roles for ACE2 include stabilization of cell adhesion through binding to integrin subunits and binding interactions with calmodulin which is thought to stabilize ACE2 at the cell surface [12,13].

Considering ACE2 function in the airway, Jia et al. demonstrated that airway tissue releases a soluble form of ACE2 (sACE2) from the cell surface into the mucosal layer, shedding occurs by proteolytic cleavage of the ectodomain from the membrane. Recently it has been shown that sACE2 can partially block SARS-CoV-2 infection of ACE2 expressing cells [14,15]. The release of sACE2 from epithelia is both constitutive and inducible [16,17]. Inducible release is instigated by several factors including inflammatory stimuli. Calmodulin inhibitors increase sACE2 production, substantiating an association between these two functions [13]. Earlier research on SARS-CoV has demonstrated that this virus can induce shedding of sACE2 protein from cells [18]. Furthermore, the SARS-CoV spike protein, independent of the virus, induced shedding of sACE2 from cells. Work by Kuba et al. showed that the SARS-CoV spike protein, injected into mice worsens acute lung failure in vivo that could be attenuated by blocking the renin-angiotensin pathway [19]. Conclusions drawn from these studies indicate that disruption of ACE2 allows elevated levels of Ang II to produce the pathological effects, described above.

In this study we utilized the air-liquid interface model of differentiation to generate airway mucociliary tissue using human nasal epithelial cells (HNECs) isolated from nasal turbinates of volunteer donors. Using cDNA generated from ALI tissue we cloned three distinct transcript variants of ACE2, each encoding a protein isoform that differs at the carboxy-terminus. Through transfection of cell lines with individual ACE2 isoforms we establish that all three ACE2 isoforms can be glycosylated, have similar cellular localization and can interact with the SARS-CoV-2 spike receptor-binding domain. Fluorescent immunohistochemistry for ACE2 on cross-sections of differentiated ALI tissue indicates heterogeneity of ACE2 protein localization. We observed ACE2 located both in the basal cell compartment and the ciliated cell compartment, but minimal signal in the central region of tissue. The apical surface of ALI tissue contains a mixture of intracellular and membrane bound ACE2 while basal cells displayed diffuse cytosolic ACE2. We also demonstrate that ALI tissue sheds ACE2 from both the apical and the basal compartments of tissue. Lastly, we show that the shedding of ACE2 proteins from ALI tissue is constitutive and unaltered by interaction with SARS-CoV-2 spike receptor binding domain. In contrast to these observations, when ACE2 isoforms are expressed in cell lines they are not constitutively shed but are released in response to SARS-CoV-2 spike. Together, our studies highlight the diverse nature of ACE2 in airway mucociliary tissue.

Methods

HNEC isolation and expansion

Detailed protocols for the isolation, growth and differentiation as well as immunohistochemistry of human nasal epithelial cells can be found in Manna and Caradonna [20]. Human nasal epithelial cells (HNECs) were isolated through brushing of inferior and middle nasal turbinates with interdental brushes (GUM). Brushes were removed from the handle and placed into an enzymatic digestion buffer (ACF Enzymatic Dissociation Solution, Stem Cell Technologies), briefly vortexed followed by incubation at 37 °C for 15 min. After digestion cells were pelleted through centrifugation at 200 x g for 5 min, pellets were suspended in basal cell expansion media (PneumaCult Ex Plus Media, Stem Cell Technologies) and incubated at 37 °C, 5%CO_2. Culture media was refreshed every two days, HNECs were collected and counted between 8 and 10 days of culture. HNECs were then either seeded directly onto transwell inserts for ALI differentiation or banked in liquid nitrogen for future experiments. Protocols for isolation of HNEC specimens from human subjects is approved by our Institutional Review Board and all donors provided informed consent.

ALI differentiation

HNECs were seeded onto semi-permeable polyester tissue culture-treated inserts that were 12 mm in diameter and 0.4 uM pore size (Corning) and cultured in expansion media until 100% confluence, confirmed by visualization of HNECs via phase contrast microscopy. Once the confluent monolayer was formed, initiation of the air-liquid interface began by removing media from the transwell insert surface and replacing the expansion media in the lower chamber with differentiation media (PneumaCult ALI Medium, StemCell Technologies). At 48 to 72 hour intervals ALI culture media was refreshed and the transwell insert was rinsed with 500 μL PBS to prevent excessive mucous accumulation. Differentiation of ALI tissue was confirmed by visualization of beating cilia via phase contrast microscopy.

ALI tissue fixation and sectioning

ALI tissue was fixed in 10% buffered formalin at 4 °C for 12–16 h then dehydrated via 20-minute graded alcohol washes (70%−80%−95%−100%). Fixed and dehydrated ALI tissue was then embedded in paraffin wax blocks for sectioning via microtome. Hematoxylin and Eosin Histological sections were deparaffinized in xylene and rehydrated via 5-minute graded alcohol washes (100%- 95%−80%−70%). Sections were placed in hematoxylin for 1 min, rinsed in tap water, dehydrated and stained with Eosin for 30 s. Lastly samples were cleared with xylene before applying coverslips. Staining was visualized and imaged via ECHO Revolve fluorescent microscope.

Immunohistochemistry

Histological sections were deparaffinized in xylene and rehydrated via 5-minute graded alcohol washes (100%- 95%−80%−70%-H2O). Antigen retrieval was performed in a digital pressure cooker (InstaPot) with slides submerged in desired antigen retrieval buffer. Sections were blocked with 5% BSA-TBST for one hour at room temperature. Primary antibodies were suspended at desired dilutions in 1% BSA-TBST and applied for one hour at room temperature, dilutions of individual antibodies can be found in table 2. Secondary antibodies conjugated to either Alexa Fluor 488 or Alexa Fluor 555 (Cell Signaling Technology) were applied at 1:1000 dilution in 1% BSA-TBST for one hour at room temperature. DAPI was applied and sections were cover-slipped and sealed. Immunofluorescence was visualized and imaged via an ECHO Revolve fluorescent microscope running the ECHO Pro-imaging application.

ACE2 protein analysis

Protein extraction for total cell extracts: Cells were washed and harvested in PBS. The cell pellet was frozen at −70 °C until use. Cells were resuspended in total cell extract/immunoprecipitation buffer (TCE/IP buffer; 50 mM Tris-Cl pH 7.5 @ 4 °C, 150 mM NaCl, 1 mM EDTA, 1% Triton X-100, protease inhibitors added immediately before use) and incubated on ice for 15 min. Cells were disrupted in a Bioruptor (diagenode, UCD 200). Settings were on high, 30 s. on and 30 s. off for 5 min. Insoluble debris was pelleted and the supernatant (TCE) used for further analysis.

Immunoprecipitation protocol

500 μg of TCE protein was added to 1 ml of TCE/IP buffer. 1 μg of antibody (Proteintech, 21,115–1-AP) was added and the solution was incubated overnight at 4 °C on a rotating platform. 20 μl of a Protein A

Table 1
.Primer Table

Primers used for the isolation of ACE2 variants
5′ primer (common to all isoforms) - CGCTCTAGAACGATGTCAAGCTCTTCCTGGCTCC
3′ primer (variant 1, 2 and X3) - CGCGCGGCCGCCTAAAAGGAGGTCTGAACATCATCAG
3′ primer (variant V3) - CGCGCGGCCGCTCAATCTTTCAAGATGGCTGTCAGCC
3′ primer (variant X2) – CGCGCGGCCGCTTACAGGCCCTTCTTCCGATCTCTGATC
Primers used to add a 6-histidine tag onto the carboxy-terminus of GFP
5′ primer – CGCGAATTCAVVATGAAGACCATCATCGCC
3′ primer – CGCGCGGCCGCTTAATGGTGATGGTGATGGTGTTTGTAGAGCTCATCCAT
qPCR primers
Actin B: 5′ - ACAGAGCCTCGCCTTTG
3′ – CCTTGCACATGCCGGAG
ACE2.v1: 5′ – CAGAAGTCAAATCCAGAGACAGA
3′ – ACAACATGGCCAAGGAGAG
ACE2.v3: 5′ – AGATCTTGATCCTCAGTTCTTGG
3′ – AGAAGCCAACTCCACTCTTG
ACE2.x2: 5′ – CAGGTTAGTAGAGGAACGAACAC
3′ - GCTAGCCTTGAACTGCCTAA

Table 2
.Antibodies utilized for the analysis of ACE2 and related proteins

ACE2 antibodies used in this study			
Catalog number	Vendor	Host species	Immunogen location
3227	ProSci Inc	Rabbit polyclonal	N-term 50 amino acids
MA5–32,307.	Invitrogen	Rabbit monoclonal	C-terminal portion
66,699–1-Ig	Proteintech.	Mouse monoclonal (IgG1)	amino acids 392–744
21,115–1-AP	Proteintech.	Rabbit polyclonal	amino acids 392–744
Other antibodies used in this study			
p63 (12,143–1-AP)	Proteintech	Rabbit polyclonal	amino acids 381–680
FoxJl (14–9965–80)	Invitrogen	Mouse monoclonal (IgG1)	mouse FOXJ1
Acetylated Tubulin (CL48866200)	Proteintech	Mouse monoclonal (IgG1) Coralite488 conjugated	not available
MUC5AC (MA5–12,178)	Invitrogen	mouse monoclonal (IgG1)	M1 mucin
GFP (50,430–2-AP)	Proteintech	Rabbit polyclonal	whole protein

sepharose (nProtein A Sepharose 4 fast flow, GE Healthcare, 17–5280–01) suspension was added and incubated for 1 hour at 4 °C on a rotator. The protein A suspension was pelleted and washed three times for 5 min each with TCE/IP buffer. Protein A pellets were resuspended in SDS-PAGE buffer and subjected to gel electrophoresis.

SDS-PAGE electrophoresis

8%−16% precast Novex Tris-Glycine gels (ThermoFisher Scientific, Waltham, MA) were used following standard protocols established in our laboratory [21].

Western blot analysis

Electrophoretically separated protein was transferred to PVDF. Standard protocols were used to perform the western blot analysis [22]. ECL chemiluminescent western blotting detection system (Amersham Corp., Buckinghamshire, UK) was used to develop positive signals. Signal acquisition was accomplished using a ThermoFisher Ibright fl1500 imaging system. Subsequent to transfer of protein to PVDF and before blocking and primary antibody, the membrane was incubated in Gentle ReView Stripping Buffer (VWR) for 30 min at 37 °C. This was followed by several washes with TBST. Addition of this step lead to a cleaner and a more intense signal.

Deglycosylation of ACE2 protein

PNGase F, which is an enzyme effective in the removal of almost all N-linked oligosaccharides from glycoproteins was purchased from New England Biolabs. The protein pellets were resuspended in 200 μl of TCE/IP buffer, divided into two equal volumes and pelleted. The pellets were treated according to vendor protocol and incubated for 1.5 h at 37 °C plus or minus PNGase F.

Cloning and transfection studies

cDNA libraries were constructed from RNA derived from HNECs grown either in submerged conditions in PneumaCult Ex Plus media or after ALI differentiation from samples taken between 15 and 25 days. RNA was isolated from cells using the NucleoSpin RNA Plus kit of Clontech Laboratories (Takara Bio Company). cDNA was constructed using the In-Fusion SMARTer Directional cDNA Library Construction kit of Takara Bio. PCR was then used to isolate clones of ACE2 using primers listed in Table 1. A common 5′ primer encoding an XbaI restriction site was used along with isoform specific 3′ primers containing a NotI restriction enzyme site. PCR amplification was accomplished with Q5 High-Fidelity DNA Polymerase from New England Biolabs. PCR products derived from the cDNA libraries were digested with the indicated enzymes and ligated into the pCINeo vector of Promega Corporation. E. coli (New England Biolabs, DH5alpha) were transformed with the ligation reactions. Individual clones were identified by colony PCR using primers within the pCINeo vector. Verification of DNA sequence was accomplished by GeneWiz (South Plainfield, NJ). HEK-293 cells (ATCC CRL-1573) and U2os cells (ATCC HTB-96) were used for transfection studies. Identified and characterized plasmids containing the ACE2 isoform open reading frames were transfected into cells using TurboFect reagent (ThermoFisher Corp.). 24 h post-transfection the cells were harvested and processed for analysis by western blot according to established procedures [22]. For fluorescence microscopy, 24-hour transfected cells were trypsinized and replated on coverslips. 24 h later the coverslips were processed for visualization. (Antibodies used; ProSci 3227, Proteintech *66,699)*.

qPCR analysis of ACE2 isoform expression in differentiating HNECs

ALI tissue was obtained at different times of differentiation. Total RNA was purified as described above and cDNA was synthesized using the Quantabio qScript cDNA Synthesis Kit from one microgram of total RNA. Two microliters of cDNA was used for qPCR using the Quantabio PerfeCta SYBR Green FastMix and the Q qPCR instrument from Quantabio. Unique primers for each of the isoforms were designed based on the strategies of Integrated DNA Technologies and obtained as PrimeTime qPCR Primers. Analysis was based on relative quantification using the software provided by Quantabio. Actin B was used as the reference gene. ΔCt values were calculated by subtracting the reference gene, actin B from each of the Ct values calculated for each of the isoforms at each time point listed.

Cycling efficiencies were consistently greater than 0.90. Melt curves for each primer pair were single, symmetrical peaks. The data presented are the averages of two independent runs for each of the time points.

Analysis of cell-independent ACE2 protein

We have developed an affinity tag to visualize ACE2 on cells as well as identify cell-independent ACE2 protein. The SARS-CoV-2 spike receptor binding domain fused to GFP was a gift from Erik Procko (Addgene plasmid # 141,184; http://n2t.net/addgene:141184; RRID:

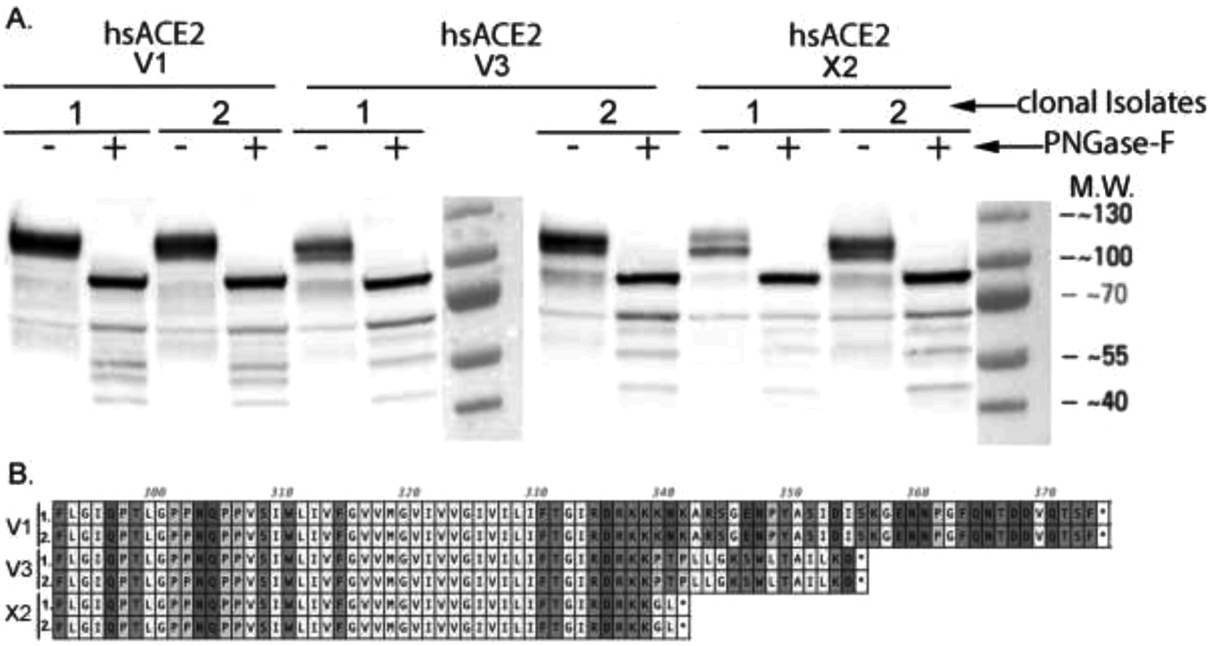

Fig. 1. *Identification of three isoforms of human ACE2.* (**A.**) cDNA isolates cloned into the plasmid expression vector, pCINeo were transfected into HEK-293. 24 h later cells were harvested, total cell extracts prepared and western blot analysis was performed on two clonal isolates from each of the three variants identified. Analysis reveals that all express protein of approximately 120 kDa. Treatment of extracts with the deglycosylating enzyme, PNGase F reveals a shift to a faster migrating band. This indicates each species can exist in a glycosylated form. (Immunostaining antibody: MmAb, Proteintech 66,699, 1:2000 dilution) (**B.**) DNA sequence analysis of each of the clonal isolates derived from the three variants indicate differences in the carboxy-terminal portion of the protein.

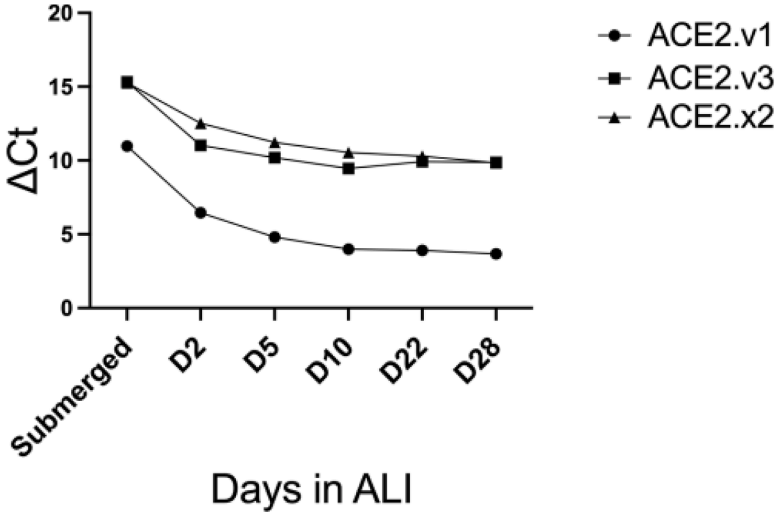

Fig. 2. *Relative gene expression of ACE2 isoforms.* RNA derived from each of these time points was subjected to reverse-transcription and quantitative PCR. ΔCt values were calculated by subtracting the reference gene, actin B from each of the Ct values calculated for each of the isoforms at each time point listed.

Addgene_141,184). Construction and characteristics of the plasmid, pcDNA3-SARS-CoV-2-S-RBD-sfGFP can be found in Chan et.al [23]. Utilizing primers described in Table 1, a 6-His tag was added onto the carboxy terminus of GFP and the HA-Spike-RBD-sfGFP-His open reading frame was re-cloned into pCINeo. The hemagglutinin (HA) leader sequence allows the fusion protein to be secreted from cells. HEK-293 cells were transfected with this construct, incubated for 48 h and observed for GFP fluorescence. At the end of this time period the media was harvested, centrifuged and subjected to chromatography using TALON Metal Affinity Resin (Takara Bio). The protein was eluted with imidazole, dialyzed and concentrated using a Millipore centrifugal filter (Amicon Ultra-15 MWCO 10 kDa).

For analysis of solubility status of the different isoforms of ACE2, U2os cells were transfected with each of the isoforms. 24 h later cells were trypsinized and replated into wells of a 12-well plate. 24 h after plating 20 μg of spike-GFP fusion protein was added to 1 ml of media and the cells were incubated at 37 °C for three hours. At this point cells were either examined for GFP fluorescence (and nuclei counterstained with NucBlue Live Cell Stain ReadyProbes Reagent, Invitrogen) or the media was harvested, centrifuged and subjected to TALON metal affinity resin pulldown. For control experiments (no incubation with spike-GFP), 20 μg of spike-GFP was added after the media was harvested and centrifuged.

To examine ACE2 protein release from HNECs, ALI cultures were established and allowed to differentiate for 25 days. Immediately preceding the addition of spike-GFP the apical and basal surfaces were

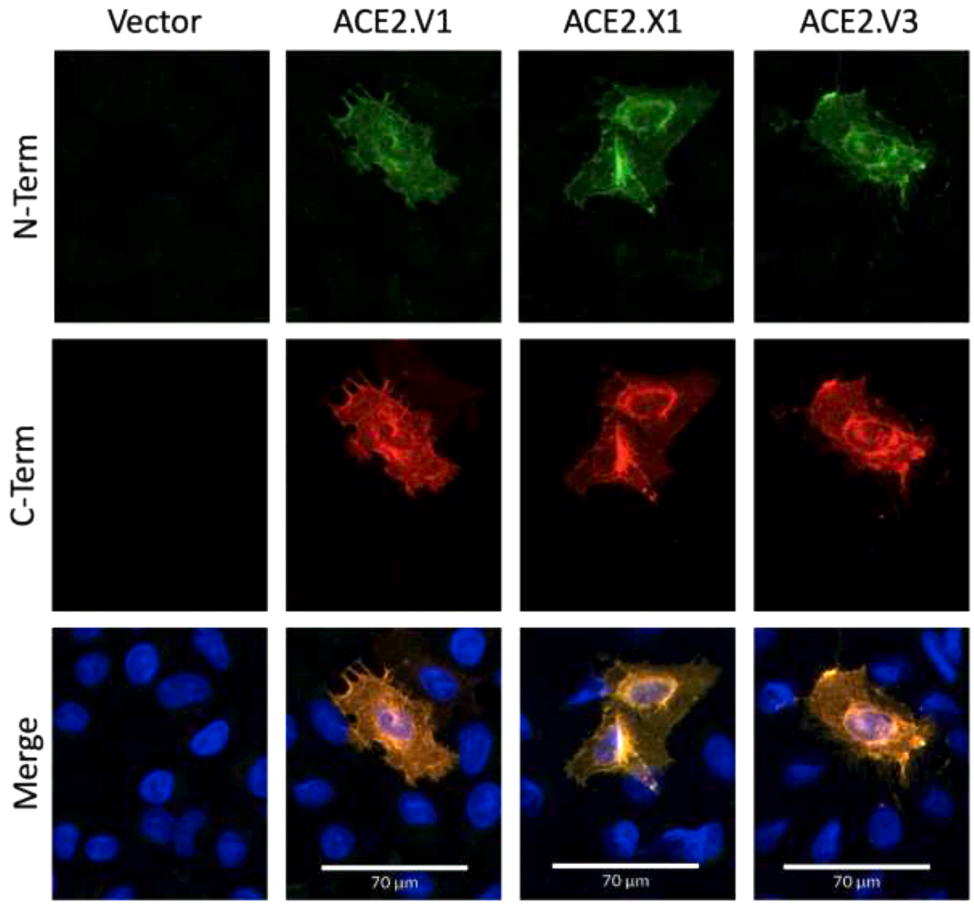

Fig. 3. *Immunofluorescence microscopy of individual isoforms of ACE2.* U2os cells were transfected with each of the isoforms of ACE2 or empty vector and then processed for immunofluorescence microscopy. As seen in the figure above, there are mostly similar patterns of localization and minor variability in perinuclear localization between isoforms. (Green: N-terminus antibody, Proteintech 66,699, 1:500 dilution. Red: C-terminus antibody (ProSci 3227, 1:250 dilution).

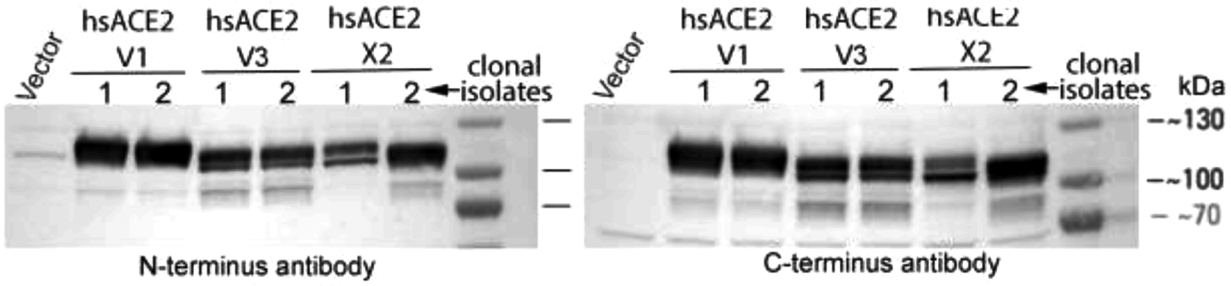

Fig. 4. *Antibody recognition of ACE2 isoforms.* Two clonal isolates for each of the three isoforms of ACE2 were analyzed by western blot using antibodies to either the N-terminal (Proteintech, 66,699) portion of the protein or the C-terminal (ProSci,3227) portion at a dilution of 1:2000.

washed 3 times with PBS. For apical shedding 20 μg of spike-GFP protein was added to the surface of the tissue contained in the trans-well inserts in 100 μl volume of PBS. For basal shedding, 20 μg of spike-GFP was added to the 1 ml of fresh ALI media below the trans-well membrane. Control (no spike-GFP) cultures were incubated with 100 μl of PBS (apical) or just fresh ALI media (basal). Cultures were allowed to incubate for 3 h at 37 °C in a 5% CO_2 incubator. Following incubation, the apical surfaces were washed with 3 × 250 μl of PBS and pooled. Media was harvested from the basal surface. The retrieved PBS and media were then centrifuged to remove cell debris (20 μg of spike-GFP was added to control samples) and subjected to TALON metal affinity resin pull-down. Western blot analysis was then performed.

The dual ADAM10 and ADAM17 protease inhibitor GW280264X (TOCRIS, a bio-techne brand) was used at a concentration of 20 μM in 100 μl of PBS placed on the apical surface of ALI cultures for 14 h [24].

Results

Identification of predicted ACE2 isoforms in ALI tissue

Genbank reports two transcript variants of human ACE2, v1 and v2 (NM_001371415 and NM_021804) which have identical coding sequence but differ in the 5′ UTR. These transcript variants will be referred to as ACE2.v1. Another transcript variant has been identified as v3 (NM_001386259). A predicted transcript variant, x2 (XM_011545551) also appears to be part of the human ACE2 gene family. Cloning primers were designed that are specific to the open-reading frames of the individual isoforms. cDNA was generated from

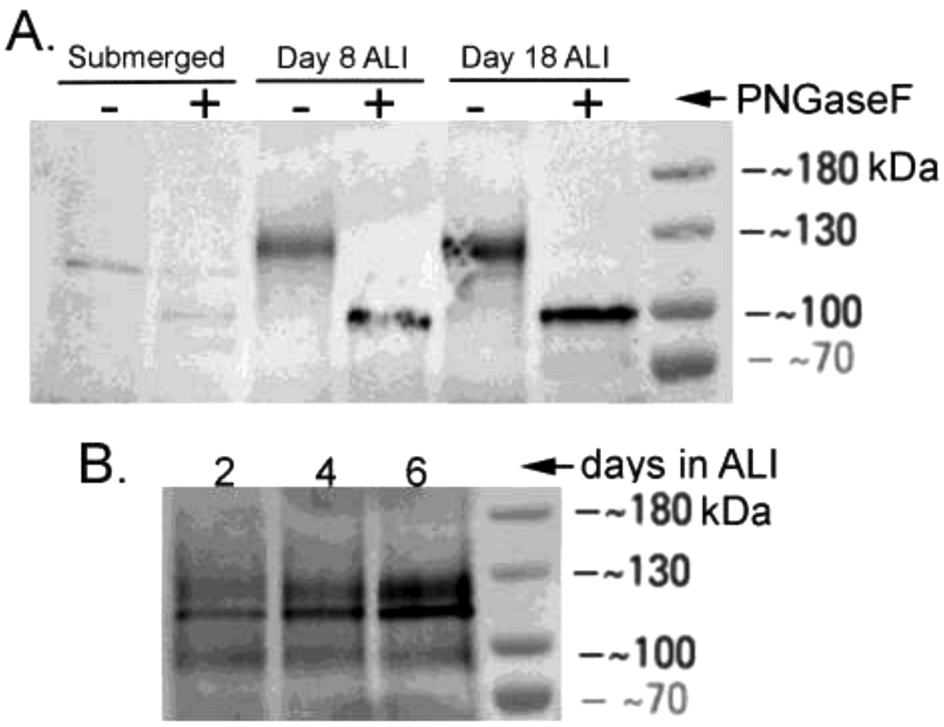

Fig. 5. *Time course of ACE2 expression in human nasal epithelial cells.* HNECs were grown submerged under media (progenitor maintenance conditions) or subjected to air-liquid interface growth conditions. Cells were harvested at the indicated times and analyzed by immunoprecipitation (RpAb, Proteintech, 21,115, 5.7 μg per IP) followed by western blot analysis (RmAb, Invitrogen, MA5–32,307, 1:500 dilution). (**A.**) As can be seen, progenitor cells do not appear to express ACE2 protein and that the process of differentiation induces expression. PNGase F treatment indicates that glycosylation of this protein is occurring during development. (**B.**) To determine when ACE2 protein expression occurs during the differentiation process, HNECs were cultured under ALI conditions. Cells were harvested at the indicated times and analyzed by immunoprecipitation and western blotting for ACE2 expression. As seen ACE2 protein is apparent by day 2 and the levels rise through days 4 and 6.

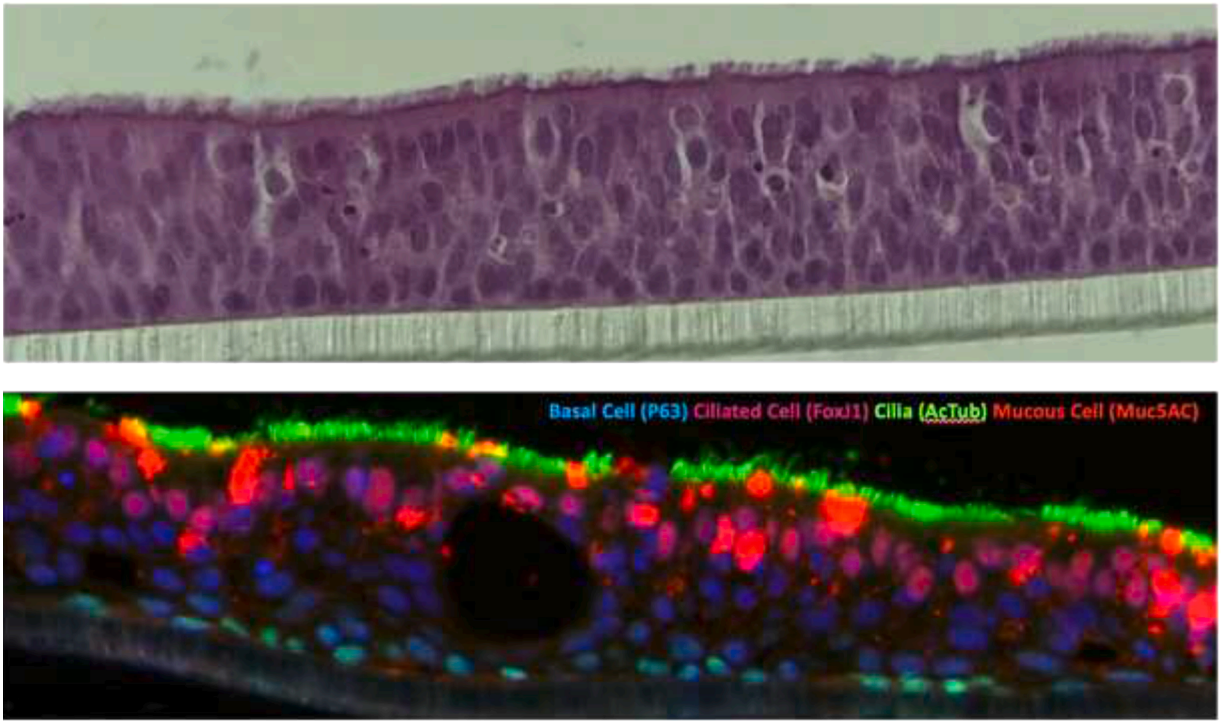

Fig. 6. *Characterization of HNEC differentiation in an air-liquid interface environment*. Upper panel is an H&E (hematoxylin and eosin) stain of differentiated HNECs. Lower panel reveals immunofluorescent identification of various cell types of the differentiated tissue.

fully differentiated HNEC ALI tissue and PCR reactions were performed with our isoform-specific primer pairs. The products were sequenced for authenticity and each was cloned into the pCINeo expression vector. These isoforms encode proteins that vary at their extreme carboxy-terminus (Fig. 1B).

Subsequent ACE2 immunoblotting of cell extracts from transfected cells revealed bands of about 120 kDa. When the cell extracts were treated with PNGase F to remove potential N-linked oligosaccharides, a shift in migration occurred to ~100 kDa indicating all three isoforms are capable of modification via glycosylation (Fig. 1A).

qPCR analysis of isoform expression in differentiating airway tissue

A more quantitative approach was taken to characterize the

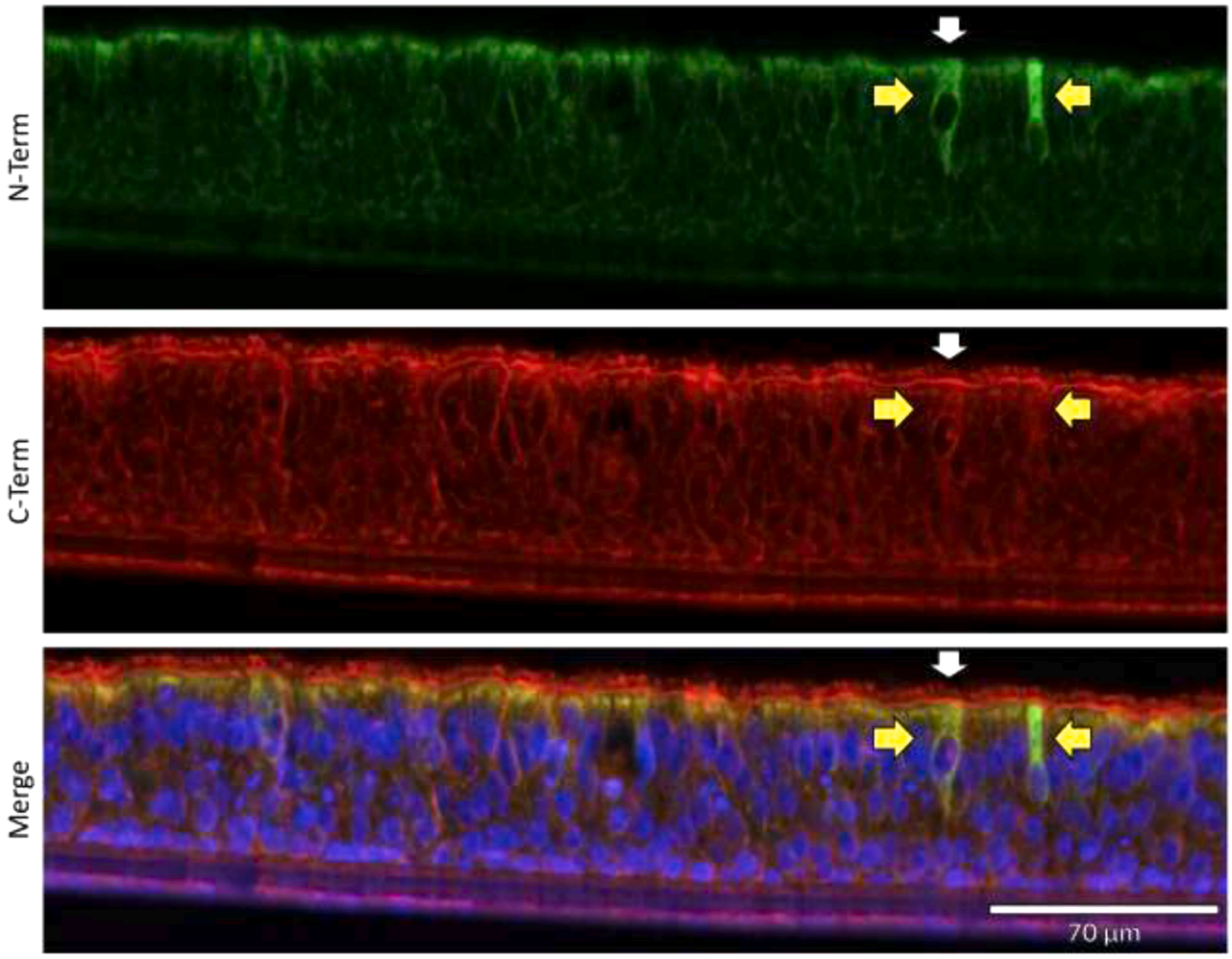

Fig. 7. *ACE2 localization utilizing fluorescent immunohistochemistry.* Two different antibodies, one to the N-terminus and the other to the C-terminal half of the protein were chosen. Although both antibodies displayed the same signals when used in our western blot analysis, they display distinct and overlapping signals via fluorescent immunohistochemistry. We observed ACE2 located both in the basal cell compartment and the ciliated cell compartment, but minimal signal in the central region of tissue. The apical cytosol of ciliated cells contained a mixture of individual signals and overlapping signals from both ACE2 antibodies (Yellow arrows highlight example of strong N-term Ab signal with minimal C-term Ab signal.) Only the ACE2 C-term antibody displayed plasma membrane signal on ciliated cells (White arrow highlights an example of C-term Ab membrane localization). ALI tissue was derived from a 34-year-old female. Bottom panel – merged image including DAPI staining of nuclei. (N-terminus Ab; ProSci 3227, C-terminus Ab; ProteinTech 66,699).

transcripts of each of these isoforms. RNA was isolated from submerged and ALI day 2 to day 28 cultures. The RNA was reverse-transcribed and quantitative PCR was performed. Analysis, utilizing a relative gene expression approach (ΔCt) revealed that expression of all three isoforms occurs during the differentiation of HNECs. ACE2.v1 appears to be the most abundant species and gene expression increases as a function of time of differentiation. ACE2.v3 and ACE2.x2 appear to be in lower abundance but do increase with time of differentiation. Design of the primer pairs utilized for this analysis was based on unique sequence within the 3′ untranslated regions of each of these isoforms, indicating that the expression patterns are specific to each of these species of RNA.

Immunofluorescent microscopy of the individual isoforms of ACE2 reveals dissimilar immunostaining patterns

Individual isoforms of ACE2 were transfected into U2os cells and visualized by immunofluorescence microscopy. As seen in Fig. 3, the isoforms appear to distribute differently within the cell. Full length ACE2.v1 localizes to the plasma membrane distributed largely as foci. In contrast ACE2.v3 and ACE2.x2 appear intracellular with an intense perinuclear distribution (Fig. 3). This data demonstrates the intrinsic ability of these isoforms to localize to different areas of the cell and may reflect differences in translational/post-translational processes or reflect differences in trafficking determinants in the individual coding sequences.

Antibodies to both the N-terminus and C-terminus of ACE2 were used in an effort to uncover any potentially masked antigenic domains of the protein. Masked domains could arise through protein-protein interactions or positional effects due to membrane localization. In order to ensure that each of the antibodies used recognized the ACE2 isoforms equally, each antibody was used in western blot analysis. As seen in Fig. 4, the three isoforms are recognized by each of the antibodies.

ACE2 expression in HNEC progenitor cells and differentiating ALI tissue

HNEC cells were analyzed by immunoprecipitation and western blot to elucidate ACE2 expression in these cells and during the differentiation phase of an ALI culture. 500 μg of progenitor cell protein extract, as well as 500 μg each of day 8 and day 18 ALI growth were subjected to immunoprecipitation and western blot analysis (Fig. 5A). Progenitor cells growing in submerged conditions (i.e., media covering the cells) do not show any ACE2 protein at the limits of detection in our system. This is consistent with our observations of ACE2 expression at the RNA level. We find minimal levels of ACE2 transcript from analysis of several cDNA

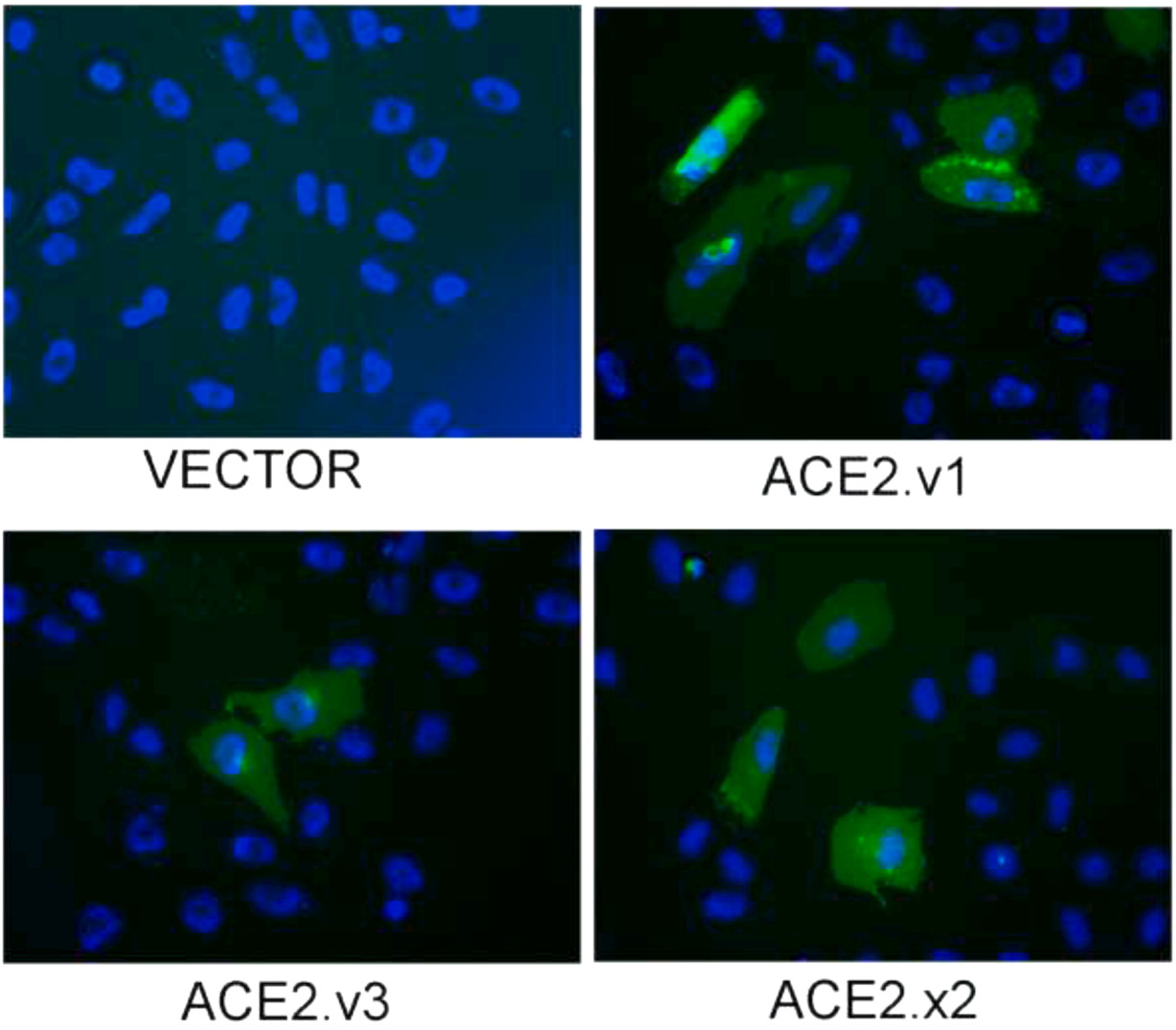

Fig. 8. *Spike-GFP binding to individual isoforms of ACE2.* U2os cells were transfected with each of the isoforms or pCINeo vector alone and 24 h later 12-well plates were reseeded with the transfected cell. After an additional 24 h 20 μg of spike-GFP protein was added to the cells for 3 h. Nuclei were stained with NucBlue live cell stain and live-cell imaging was accomplished using an Echo Revolve microscope. As seen in the figure no GFP fluorescence is seen in the vector control indicating minimal nonspecific binding. The three isoforms reveal similar binding and have generalized cell-surface GFP fluorescence.

libraries constructed from progenitor HNECs that were grown under submerged conditions. This work verifies earlier findings indicating little to no expression of ACE2 in airway basal cells (33). However, when HNEC progenitor cells are exposed to an air-liquid interface for 8 days ACE2 protein becomes apparent. This data indicates that HNEC cells, when maintained under progenitor conditions, express minimal to no ACE2 protein. Analysis of a shorter time-course of ALI growth reveals that ACE2 expression begins at least at day 2 and increases thereafter (Fig. 5B).

ACE2 protein appears to be both intracellular and membrane-bound in ALI tissue

HNEC differentiation in an air-liquid interface environment produces the characteristic cell types seen in vivo situations. Full differentiation occurs around day 20 as seen in Fig. 6. Antibodies used for immunofluorescent imaging reveal the various cell types associated with the differentiated tissue. These include basal progenitor cells (p63 positive), ciliated cells (FoxJ1) with associated cilia (Acetylated Tubulin, AcTub) and mucous cells (Muc5AC).

For our analysis of ACE2 protein we continued to use two different antibodies, one to the N-terminus (ProSci 3227) and the other to the C-terminus region (ProteinTech 66,699). Although the two antibodies displayed the same band pattern when used in our western blot analyses, they surprisingly exhibited distinct and overlapping patterns via fluorescent immunohistochemistry of ALI tissue. Each antibody displayed intracellular signals in the apical surface of ALI tissue but only the ACE2 C-term antibody exhibited plasma membrane localization. In the basal cell compartment, we detected ACE2 localized intracellularly at the basolateral region of cells (Fig. 7).

The receptor binding domain of SARS-CoV-2 spike protein induces the release of ACE2 protein isoforms from U2os transfected cells

In an effort to further analyze adherent and cell-independent forms of ACE2, advantage was taken of the SARS-CoV-2 spike receptor binding domain. The original construct containing the spike (RBD)-GFP was provided through Addgene by Chan and collaborators [23]. The construct was modified to contain a six-histidine tag at the C-terminus of the GFP protein. In addition to providing a relatively easy means of purifying spike-GFP, this 6-his tag created a simple means of extracting cell-free ACE2 from solution. As seen in Fig. 8, spike RBD binds equally well to all three isoforms of ACE2.

Previous research as outlined in the introduction indicate that ACE2

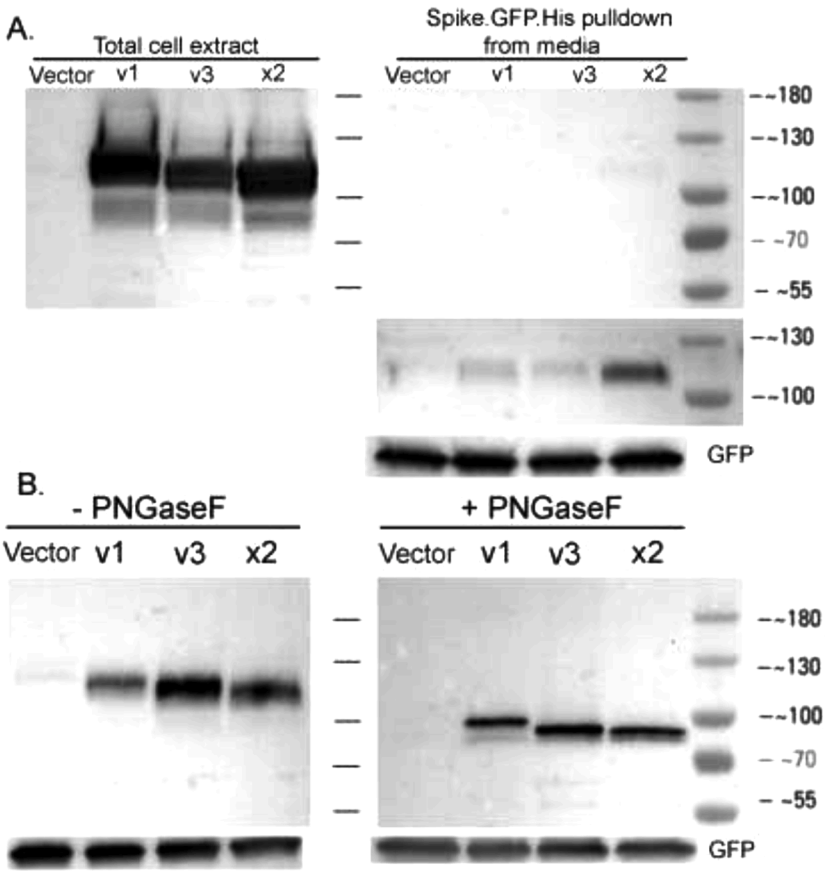

Fig. 9. *Analysis of ACE2 release from isoform transfected U2os cells.* (**A**) Left panel is a western blot of total extracted protein (30 μg) from individual isoform transfected cells. Right panel is media derived from the transfected cells and subjected to spike-GFP pulldown procedures. Both left and right blots were imaged for 15 s. The lower right panel is a longer exposure (10 min) indicating that minimal release occurs in the over-expressing cells and also indicates little to no apparent contamination with cell-associated ACE2. Panel labeled GFP indicates equivalent amounts of spike-GFP were used in each pulldown. (**B**) Transfected cells were incubated with spike-GFP for three hours and then subjected to affinity pull-down procedures. As seen, significant sACE2 appears to be released from each of the transfectants. Left and right panels indicate the presence and removal of glycosyl moieties of ACE2, respectively. Imaged for 2 min. *Vector - pCINeo vector alone. (ACE2-RmAb: Invitrogen MA5–32,307, 1:500 dilution).*

can be shed either constitutively or through induction by various agents, including coronavirus spike proteins [16] [17]. The individual isoforms of ACE2 were analyzed for release from cells. As indicated in Fig. 9A, minimal release occurs from cells transfected with the isoforms in the absence of any stimulus such as spike protein. In contrast incubation of the transfected cells with spike-GFP for three hours induced significant shedding of each of the isoforms.

The cell-free nature of apical and basal ACE2 in differentiated airway epithelia

In an attempt to uncover characteristics of ACE2 release in airway epithelia, 25-day old ALI cultures were incubated with spike-GFP fusion protein and compared to untreated controls. As seen in Fig. 10, unstimulated release of ACE2 protein occurs from both the apical and basal surfaces of the control ALI cultures. The spike-GFP protein does not appear to augment release, at least under the conditions that were analyzed here. What is also evident is that the apical and basal forms of ACE2 appear to be slightly different in terms of migration in SDS-PAGE. This is most apparent in the PNGase F treated samples (Fig. 10B). This may suggest differential location of individual isoforms of ACE2. The multiple bands seen, particularly with the PNGase F samples may indicate partial de-glycosylation, O-linked glycosyl moieties, which are resistant to PNGase F treatment. Alternatively, it may indicate differential proteolytic processing by different proteases. The Adam17 protease produces an ectodomain product for ACE2 of about 70–75 kDa [25], whereas TMPRSS2 protease yields an ectodomain ACE2 species of about 80–85 kDa. It should be noted that previous studies demonstrate that TMPRSS2 does not appear to cause ACE2 shedding [26].

In an attempt to determine whether the 70 kDa band seen in Fig. 10B is a proteolytic product, we utilized an inhibitor of ADAM17 which also inhibits another protease, ADAM10. As seen in Fig. 10C, treatment of ALI tissue with the inhibitor results in a diminished amount of the 70 kDa band. This putatively indicates that the 70 kDa species is a proteolytic species produced by proteolytic cleavage. At present we do not understand why the middle band seen in Fig. 10B is absent from 10C. It may be differential epitope recognition due to different lots of antibody that was used between Fig. 10B and 10C.

Discussion

Full-length ACE2 (variants 1/2) and two additional isoforms were cloned from well differentiated ALI tissues derived from two independent donors (Female age 34, Male age 33). This study identified and cloned transcripts for two additional ACE2 isoforms, v3 and x2. Whether or not these isoforms are specific to the airway is still to be determined. It is important to note that these two alternate transcript variants of full length ACE2 have unique residues (Fig. 1) at their extreme C-termini and are not mere truncations through exon deletion. Since each ACE2 isoform, including full-length, contain unique C-term protein motifs this indicates the possibility that each ACE2 isoform may possess a unique function. Our study has demonstrated that each of these ACE2 isoforms is capable of being glycosylated, each has similar cellular localization, each is capable of interaction with the SARS-CoV-2 spike protein, and each can be shed from the cell as a soluble protein.

Quantitative PCR was used to corroborate expression of the ACE2 isoforms. As seen in Fig. 2, all three transcripts are detected. Submerged cultures of HNECs have very low levels of message. This reflects what we see at the protein level for submerged cultures (Fig. 5). As differentiation proceeds, message abundance for all three isoforms increases. ACE2.v1 appears to be the most abundant transcript throughout differentiation.

To increase the rigor of our study we utilized multiple ACE2 antibodies largely directed to opposite regions of the protein (N-terminus and C-terminus) for our immunoblotting and immunofluorescent

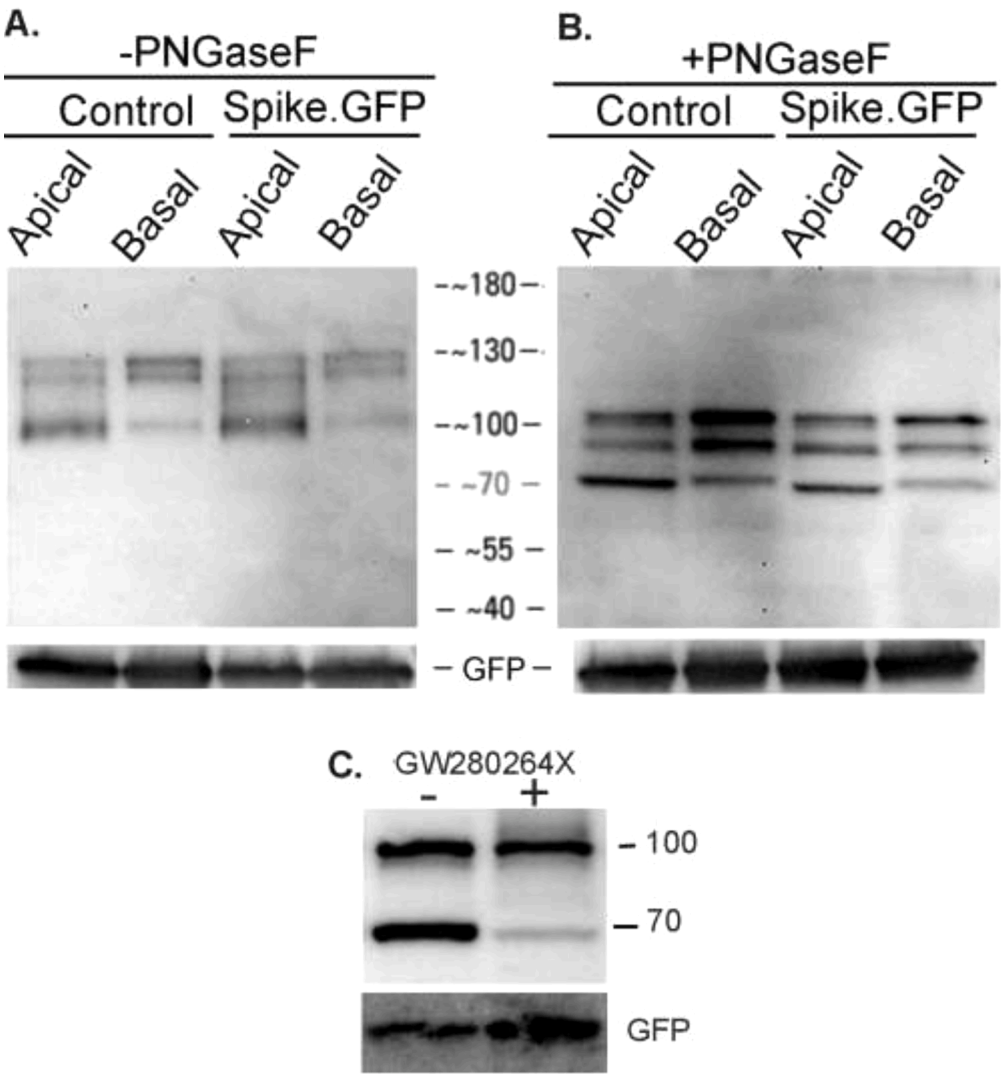

Fig. 10. *Apical and basal nature of ACE2.* 25-day ALI cultures were exposed to 20 μg of spike-GFP fusion protein, either apically or at the basal surface for 3 h at 37 #x00B0; C in a 5% CO_2 incubator. At the end of the incubation samples were harvested, centrifuged and subjected to affinity pull-down. Control indicates PBS alone (apical) or media alone (basal). Control PBS and media were harvested, centrifuged and then 20 μg of spike-GFP protein was added and ACE2 was then affinity isolated. (**A.**) As indicated in the figure it appears that ACE2 is released in the absence of any inducing agent. Equivalent amounts of ACE2 are seen in the absence or presence of spike-GFP protein. (**B.**) Affinity isolated samples were treated with PNGase F. There are slight differences in ACE2 gel migration between isolates derived from the apical and basal surfaces. (**C.**) ALI cultures were incubated without or with 20 μM GW280264X, a dual ADAM10 and ADAM17 protease inhibitor for 14 h on the apical surface and processed as described above. As seen in the figure, the protease inhibitor decreases the amount of the 70 kg dalton band. This is indicative of protease-dependent shedding of the ACE2 protein. *(ACE2-RmAb: Invitrogen MA5–32,307, 1:500 dilution). Imaged for 2.5 min.*

analyses. When single ACE2 isoforms were transfected into either HEK293 or U2os cells and subsequent cell lysates were immunoblotted for ACE2, both antibodies gave identical signals (Fig. 4), indicating that both epitopes are recognized on every isoform. Immunofluorescence for ACE2 in transfected cells revealed that full length ACE2.v1 localized to the plasma membrane. ACE2 v3 and x2 also localized to the plasma membrane but at a reduced intensity with many less foci (Fig. 3). In contrast to v1 both v3 and x2 showed an increased frequency of perinuclear staining, which may indicate increased residence in the endoplasmic reticulum or golgi due to alternate translational/post-translational pathways. Despite these studies being performed in an immortalized cell line rather than the primary airway cells that they were cloned from, the data demonstrates the intrinsic ability of these isoforms to localize to similar areas of the cell, namely intracellularly and the plasma membrane.

Our investigations using HNECs cultured in self-renewing conditions revealed little to no ACE2 transcript or protein expression. We found that ACE2 transcript and protein expression was induced within 48 h of initiation of ALI culture, and expression continued to increase throughout differentiation. We believe it's possible that ACE2 may have a unique function within the early stages of airway progenitor cell differentiation and subsequent regeneration of mucociliary tissue. To this end, it would be pragmatic for future studies to aim at determining if ALI tissue can develop properly without adequate levels of ACE2 protein.

An additional finding from these results was our immunofluorescent studies with fully differentiated ALI tissue which revealed that the two antibodies give distinct and overlapping patterns (Fig. 7). Previous studies have shown that ACE2 protein localizes within the plasma membrane of ciliated cells [27]. We corroborated those observations and expanded on them by demonstrating ACE2 protein is also found intracellularly within ciliated cells. Interestingly, we discovered plasma membrane ACE2 is only observed using the antibody towards the C-terminus region, suggesting that the epitope for the N-terminus antibody is blocked, possibly through an association with some unknown partner. Furthermore, the intracellular region of ciliated cells exhibited green and yellow signals, corresponding to the N-terminus (Green) and an overlap of both N-term/C-term signals (Yellow). Altogether, the ciliated cells in ALI tissue displayed two areas of ACE2 localization with three distinct ACE2 signals (Intracellular/Green/N-term, Intracellular/Yellow/ N-term/C-term, Membrane/Red/C-term).

One explanation for the IHC patterns we observed in multiciliated cells (Fig. 7) could be that the distinct staining patterns are ACE2 in different stages of maturation or recycling and that at each stage a distinct region of the ACE2 protein interacts with a specific partner, precluding antibody recognition of that epitope. Our IHC analysis also revealed ACE2 localized within the intracellular region of most basal progenitor cells. We found it notably interesting that the progenitor cells express ACE2 upon initiation of differentiation, throughout differentiation and during homeostasis, highlighting again our hypothesis that ACE2 possesses progenitor-specific activity.

In an effort to monitor the cellular release of ACE2, we took advantage of the SARS-CoV-2 spike protein. Modifying an expression vector constructed by Chan et al. [23], we performed an analysis of ACE2, first from isoform transfected cells and then from well-differentiated HNEC cultures. Fig. 8 demonstrates uniform binding of the spike protein to transfected cells. Each isoform appears equivalent in spike binding. In order to determine the cell-free status of ACE2, media was isolated from 48-hour transfected cultures and the spike-GFP fusion protein was added to the conditioned media to selectively isolate ACE2 using metal affinity protocols. As seen in Fig. 9 very little ACE2 appears to be released from cells for any of the isoforms in unperturbed conditions (Fig. 9A). When 48-hour transfectants were incubated with spike-GFP for 3 h prior to ACE2 purification from conditioned media, significant release of soluble ACE2 is seen for all the isoforms (Fig. 9B). This corroborates previous work with SARS-CoV in studies that use immortalized cells in culture recently reviewed in [28,29].

We next examined the release of ACE2 in 25-day ALI cultures. Data shown in Fig. 10 demonstrates that ACE2 is constitutively released from both the apical and basal surfaces of the cultures. Surprisingly, incubation with the spike-GFP fusion construct did not alter the release of ACE2 from either the apical or basal surface of these differentiated airway cultures. This is in contrast to what is seen with ACE2 transfected cells (Fig. 9). What is also noted in Fig. 10 is that there are minor molecular weight differences of ACE2 recovered from the apical and basal surfaces. This is especially evident when the affinity isolated proteins are subjected to glycosyl-moiety removal with PNGase F (Fig. 10B). This variation may indicate differential isoform location between apical and basal surfaces. In an attempt to identify protease-released ACE2, ALI cultures were incubated with the dual ADAM10/ADAM17 protease inhibitor. As seen in Fig. 10C the 70 kDa band shows a significant decrease in intensity relative to control. This indicates that this species of ACE2 is proteolytically shed.

As indicated above, airway shedding of ACE2 may provide a protective environment from initial SARS-CoV-2 infection. It would be essential to understand the kinetics of unperturbed ACE2 shedding as well as understanding what endogenous or exogenous factors exist that may alter the kinetics of shedding. Our investigations uncovered discrepancies between steady-state ACE2 release in ALI tissue versus transfected cell-lines. It is our belief that the constitutive release of ACE2 observed in ALI tissue is the biologically relevant form of in-vivo ACE2 solubilization as ALI tissues share the cell types and structure of in-vivo airway mucociliary tissue and are generated by primary, untransformed airway progenitor cells. Future investigations into the mechanisms of ACE2 membrane release should take special consideration as to the model system chosen.

We detected three distinct molecular weight species of ACE2 being shed from ALI tissue (Fig. 10, +PNGase F). It is possible that each of the ACE2 bands represent a different proteolytic species of ACE2 shed via different pathways, or that each band represents unique post-translational modifications that shift migration on SDS-PAGE. Alternatively, some of these ACE2 species may be associated with extracellular vesicles such as exosomes. This is based on unpublished observations in our lab that the spike-GFP affinity pulldown fractions also contain the exosome marker Alix, a cargo sorting ESCRT-associated protein [30]. Intriguingly CD68 was also found associated with the spike-ACE2 affinity isolated fractions. CD68 is a glycosylated type I transmembrane protein highly expressed on macrophages and other mononuclear phagocytes and is associated with inflammatory responses [31] [32]. Further research is required to confirm these initial findings.

We also detected ACE2 in conditioned media collected from the basal compartment of ALI cultures. We believe this ACE2 originated from the basal progenitor layer as our IHC analysis revealed ACE2 expression in the basal compartment and little to no expression in the central region of ALI tissue. It is sensible to assume that ACE2 would be released from the basal compartment of airway mucociliary tissue as this would allow access to the bloodstream via capillaries of the lamina propria. It is also noteworthy that there were slight differences in the observed molecular weight of released ACE2 derived from the apical versus basal compartment of ALI tissues. These minor differences in SDS-PAGE migration are similar to the differences observed between the individual ACE2 isoforms when they are transiently transfected into cell lines. Current understanding is that cell-free ACE2 can be created by protease cleavage at the membrane, releasing the ectodomain of the protein [28,29]. Since the differences between the isoforms are at the extreme carboxy-terminus, the differences should be removed with release of the ectodomain. Yet for both, the recombinant ACE2 isoforms expressed through transfection and the examination of released ACE2 from the apical and basal surfaces of differentiated HNECs, differences in migration remain. This leaves us with the tentative conclusion that the different carboxy-domains direct ACE2 to different post-translational fates. This could be confirmed with future investigations using RNA-FISH on differentiated ALI tissue to visualize the tissue location of the individual ACE2 transcript variants to determine if transcription is specific to certain cell types of the airway. Delineating novel functions of ACE2 in the basal progenitor compartment of airway mucociliary tissue is fundamental in understanding how to counteract the disruption of airway tissue homeostasis caused by SARS-CoV-2 infection.

Pertaining to what the distinct roles of isoforms may be, previous studies demonstrated that sACE2 maintains the ability to catabolize angiotensin II, suggesting that membrane bound or sACE2 can potentially function in the resolution of inflammation in the airway (20). Membrane bound ACE2 has been observed to function in cellular adhesion through interactions with integrins, indicating another potential role in airway tissue (29). There is also the fascinating potential for undiscovered airway-specific substrates and functions of individual ACE2 isoforms. Another consideration for ACE2 status is the amount of sACE2 protein released from the plasma membrane into the mucosal layer. Previous studies demonstrated that sACE2 interacts with the SARS-CoV spike protein and that increasing the concentration of sACE2 conferred resistance to experimental SARS-CoV infection. The group also determined that ACE2 must be membrane-bound to facilitate entry of the SARS-CoV pathogen (34). These studies support the postulate that having high concentrations of sACE2 in the airway mucous layer will confer some level of resistance to SARS-CoV-2 infection, as each sACE2 protein would in essence act as a ‘sponge’ for a viral particle.

Expanding on this hypothesis, the consequence for an individual having high levels of membrane bound ACE2 is an increase in available entry points for viral particles and thereby an increase in susceptibility to SARS-CoV-2 infection. It is conceivable that the wide variability in the severity of COVID-19 cases lie within the airway ACE2 status of the patients. Contributing to whether ACE2 is a functional target for SARS-CoV-2 include the potential for differential isoform expression, altered distribution in the cell between membrane-bound, intracellular or the secreted form as well as differences in post-translational modification. It is in the interest of public health to understand how these ACE2 parameters affect the susceptibility of airway tissue to SARS-Cov-2 infection, in addition to the potential impact that diet, environment, genetics, prescription and over-the-counter medications may have on modulating these ACE2 parameters. Perhaps there are readily available, FDA-approved solutions that can help decrease susceptibility to COVID-19.

Declaration of Competing Interest

The authors declare no conflicts of interest.

References

[1] P. Zhou, et al., A pneumonia outbreak associated with a new coronavirus of probable bat origin, Nature 579 (7798) (2020) 270–273.
[2] S.R. Tipnis, et al., A human homolog of angiotensin-converting enzyme. Cloning and functional expression as a captopril-insensitive carboxypeptidase, J. Biol. Chem. 275 (43) (2000) 33238–33243.

[3] S. Lukassen, et al., SARS-CoV-2 receptor ACE2 and TMPRSS2 are primarily expressed in bronchial transient secretory cells, EMBO J. 39 (10) (2020), e105114.
[4] C. Tikellis, M.C. Thomas, Angiotensin-Converting Enzyme 2 (ACE2) is a key modulator of the renin angiotensin system in health and disease, Int. J. Pept. 2012 (2012), 256294.
[5] C. Vickers, et al., Hydrolysis of biological peptides by human angiotensin-converting enzyme-related carboxypeptidase, J. Biol. Chem. 277 (17) (2002) 14838–14843.
[6] R.A. Santos, et al., Angiotensin-(1-7) is an endogenous ligand for the G protein-coupled receptor Mas, Proc. Natl. Acad. Sci. U. S. A. 100 (14) (2003) 8258–8263.
[7] R.R. Gaddam, S. Chambers, M. Bhatia, ACE and ACE2 in inflammation: a tale of two enzymes, Inflamm. Allergy Drug Targets 13 (4) (2014) 224–234.
[8] S. Vukelic, K.K. Griendling, Angiotensin II, from vasoconstrictor to growth factor: a paradigm shift, Circ. Res. 114 (5) (2014) 754–757.
[9] Y. Qi, et al., Lentivirus-mediated overexpression of angiotensin-(1-7) attenuated ischaemia-induced cardiac pathophysiology, Exp. Physiol. 96 (9) (2011) 863–874.
[10] Y. Imai, et al., Angiotensin-converting enzyme 2 protects from severe acute lung failure, Nature 436 (7047) (2005) 112–116.
[11] M. Oz, D.E. Lorke, Multifunctional angiotensin converting enzyme 2, the SARS-CoV-2 entry receptor, and critical appraisal of its role in acute lung injury, Biomed. Pharmacother. 136 (2021), 111193.
[12] N.E. Clarke, et al., Angiotensin converting enzyme (ACE) and ACE2 bind integrins and ACE2 regulates integrin signalling, PLoS ONE 7 (4) (2012) e34747.
[13] D.W. Lambert, et al., Calmodulin interacts with angiotensin-converting enzyme-2 (ACE2) and inhibits shedding of its ectodomain, FEBS Lett. 582 (2) (2008) 385–390.
[14] W. Tai, et al., Characterization of the receptor-binding domain (RBD) of 2019 novel coronavirus: implication for development of RBD protein as a viral attachment inhibitor and vaccine, Cell Mol. Immunol. (2020).
[15] V. Monteil, et al., Inhibition of SARS-CoV-2 infections in engineered human tissues using clinical-grade soluble human ACE2, Cell 181 (4) (2020), 905–913 e7.
[16] H.P. Jia, et al., ACE2 receptor expression and severe acute respiratory syndrome coronavirus infection depend on differentiation of human airway epithelia, J. Virol. 79 (23) (2005) 14614–14621.
[17] H.P. Jia, et al., Ectodomain shedding of angiotensin converting enzyme 2 in human airway epithelia, Am. J. Physiol. Lung Cell. Mol. Physiol. 297 (1) (2009) L84–L96.
[18] I. Glowacka, et al., Differential downregulation of ACE2 by the spike proteins of severe acute respiratory syndrome coronavirus and human coronavirus NL63, J. Virol. 84 (2) (2010) 1198–1205.
[19] K. Kuba, et al., A crucial role of angiotensin converting enzyme 2 (ACE2) in SARS coronavirus-induced lung injury, Nat. Med. 11 (8) (2005) 875–879.
[20] V. Manna, S. Caradonna, Isolation, expansion, differentiation, and histological processing of human nasal epithelial cells, STAR Protoc. 2 (4) (2021), 100782.
[21] S.M. Rotoli, S.J. Caradonna, Combining Non-reducing SDS-PAGE analysis and chemical crosslinking to detect multimeric complexes stabilized by disulfide linkages in mammalian cells in culture, J. Vis. Exp. (147) (2019).
[22] S.M. Rotoli, J.L. Jones, S.J. Caradonna, Cysteine residues contribute to the dimerization and enzymatic activity of human nuclear dUTP nucleotidohydrolase (nDut), Protein. Sci. 27 (10) (2018) 1797–1809.
[23] K.K. Chan, et al., Engineering human ACE2 to optimize binding to the spike protein of SARS coronavirus 2, Science 369 (6508) (2020) 1261–1265.
[24] J. Yang, et al., ADAM10 and ADAM17 proteases mediate proinflammatory cytokine-induced and constitutive cleavage of endomucin from the endothelial surface, J. Biol. Chem. 295 (19) (2020) 6641–6651.
[25] M. Iwata, J.E. Silva Enciso, B.H. Greenberg, Selective and specific regulation of ectodomain shedding of angiotensin-converting enzyme 2 by tumor necrosis factor alpha-converting enzyme, Am. J. Physiol. Cell Physiol. 297 (5) (2009) C1318–C1329.
[26] A. Heurich, et al., TMPRSS2 and ADAM17 cleave ACE2 differentially and only proteolysis by TMPRSS2 augments entry driven by the severe acute respiratory syndrome coronavirus spike protein, J. Virol. 88 (2) (2014) 1293–1307.
[27] A.C. Sims, et al., Severe acute respiratory syndrome coronavirus infection of human ciliated airway epithelia: role of ciliated cells in viral spread in the conducting airways of the lungs, J. Virol. 79 (24) (2005) 15511–15524.
[28] S.M. Gonzalez, A.B. Siddik, R.C. Su, Regulated Intramembrane proteolysis of ACE2: a potential mechanism contributing to COVID-19 pathogenesis? Front. Immunol. 12 (2021), 612807.
[29] H.C. Yalcin, et al., Do changes in ACE-2 expression affect SARS-CoV-2 virulence and related complications: a closer look into membrane-bound and soluble forms, Int. J. Mol. Sci. 22 (13) (2021).
[30] G. Raposo, W. Stoorvogel, Extracellular vesicles: exosomes, microvesicles, and friends, J. Cell Biol. 200 (4) (2013) 373–383.
[31] D.A. Chistiakov, et al., CD68/macrosialin: not just a histochemical marker, Lab. Invest. 97 (1) (2017) 4–13.
[[32] M. Osada-Oka, et al., Macrophage-derived exosomes induce inflammatory factors in endothelial cells under hypertensive conditions, Hypertens. Res. 40 (4) (2017) 353–360.